Probabilistic Joint Interpretation of Geoelectrical and Seismic Data for Landfill Characterization

Itzel Isunza Manrique[1], David Caterina[1], Thomas Hermans[2] and Frederic Nguyen[1]

[1] Applied Geophysics Department, Urban and Environmental Engineering, University of Liege, Belgium. [2] Geology Department, Ghent University, Ghent, Belgium. Corresponding author: iisunza@uliege.be

1) Motivation

RAWFILL project: supporting a new circular economy for RAW materials recovered from landFILLs.

SPAQuE · OVAM · LIÈGE université · British Geological Survey
atrasol · BAV · LES CHAMPS JOUBERT · Cleantech Flanders

Geophysical characterization (multiple methods)
↓
Optimized sampling survey
↓
Geophysical calibration
↓
Resource distribution model

4) Probabilistic approach

What structural information of the landfill is delivered with each method?

- ERT → Shallowest zone of the cover layer, saturated zones
- IP → Upper limit of the waste body
- MASW + HV → Lower limit of the waste

To assess the ability of these methods to identify the layers of the landfill we follow the probabilistic approach proposed by Hermans and Irving, 2017:

1. Compare the inverted models with the co-located data from the trenches through the computation of histograms for each layer. The S-wave cannot resolve the 4 upper layers, only the transition between waste and natural soil.
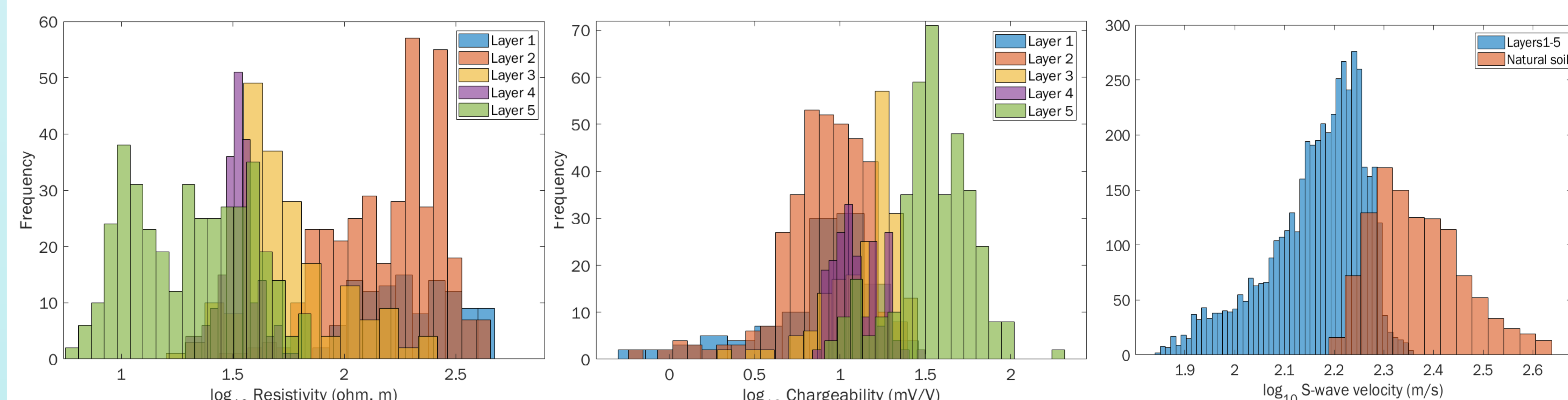
Fig. 6. Histograms of the resistivity model (left) and chargeability (in the middle) for each of the 5 layers identified in the excavations. On the right, the histogram of the S-wave velocity for layers 1-5 together (as they could not be resolved with MASW) and the natural soil. Layer 5 is the MSW body.

2. Select the model(s) that can better resolve a specific structure of the landfill and compute the conditional probabilities. As we wanted to delineate the vertical extent of the waste, we selected the chargeability and the S-wave models. Sensitivity correction ERT/IP: we used Bayes' rule to compute sensitivity-dependent ERT/IP distributions (i.e. conditional probability given ERT/IP and sensitivity).
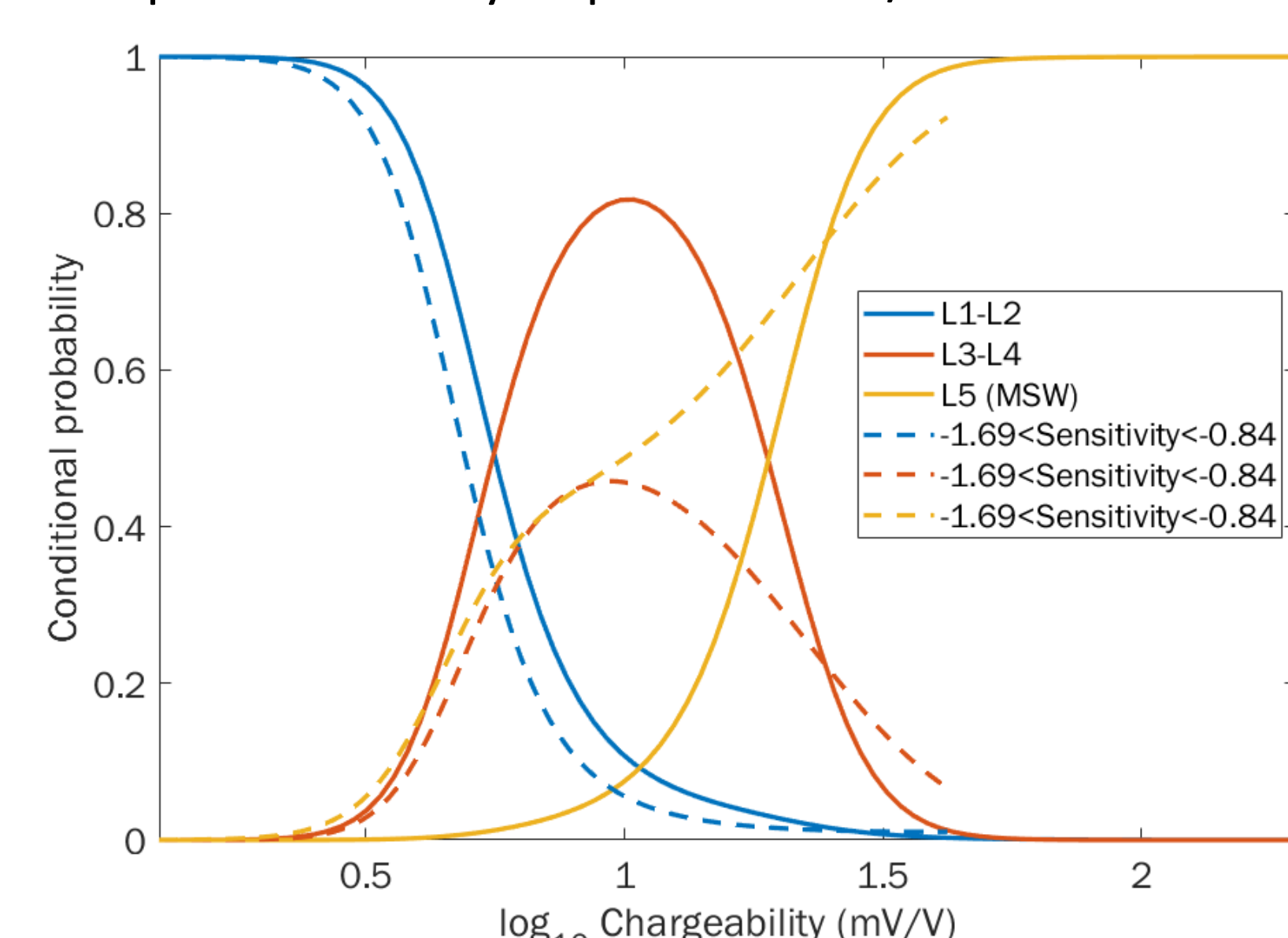
Fig. 6. Conditional probability of layers 1-2, layers 3-4 and layer 5 given the chargeability (solid lines). Conditional probabilities of the same sets of layers given the chargeability and a sensitivity range between -1.69 and -0.84.
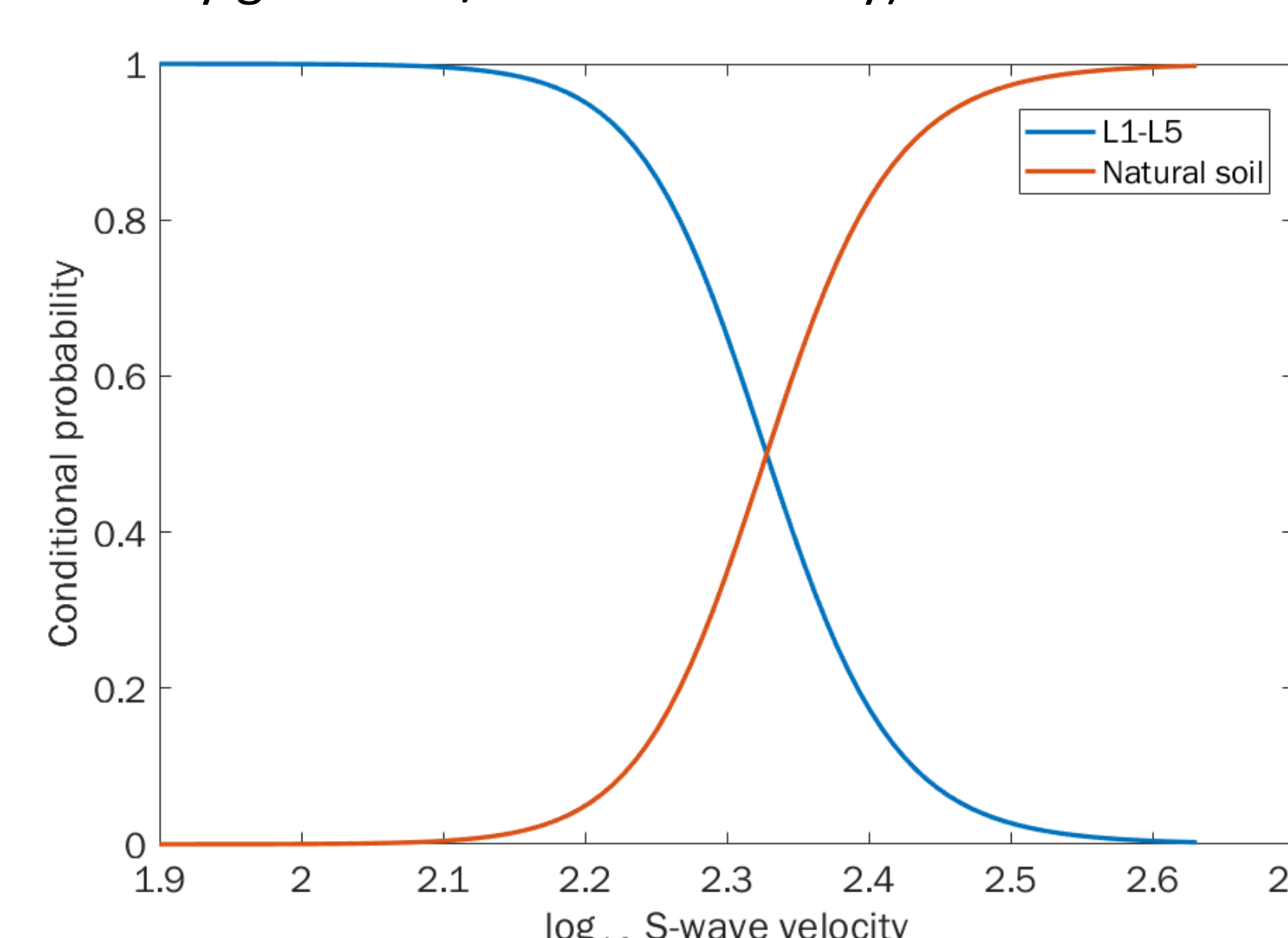
Fig. 7. Conditional probability of layers 1-5 and natural soil given the S-wave velocity.

2) Case study

Survey: Within the RAWFILL project, we investigated a municipal solid waste landfill (MSW) located in Meerhout (Belgium), active from 1962 to 1998, using a multi-geophysical approach. Selected methods include frequency-domain electromagnetic induction (EMI), magnetometry, electrical resistivity tomography (ERT), induced polarization (IP), ground penetrating radar (GPR) and seismic methods. Data collected were used to design a guided sampling with 9 boreholes and 7 trial pits. In this contribution, we focus in one area of the site along one profile where we acquired co-located ERT/IP data, partially co-located multiple analysis of surface waves (MASW) data and 3 Horizontal to vertical (H/V) spectral ratio measurements. In this profile 7 trial pits and 1 borehole were excavated (see locations in Figure 1).
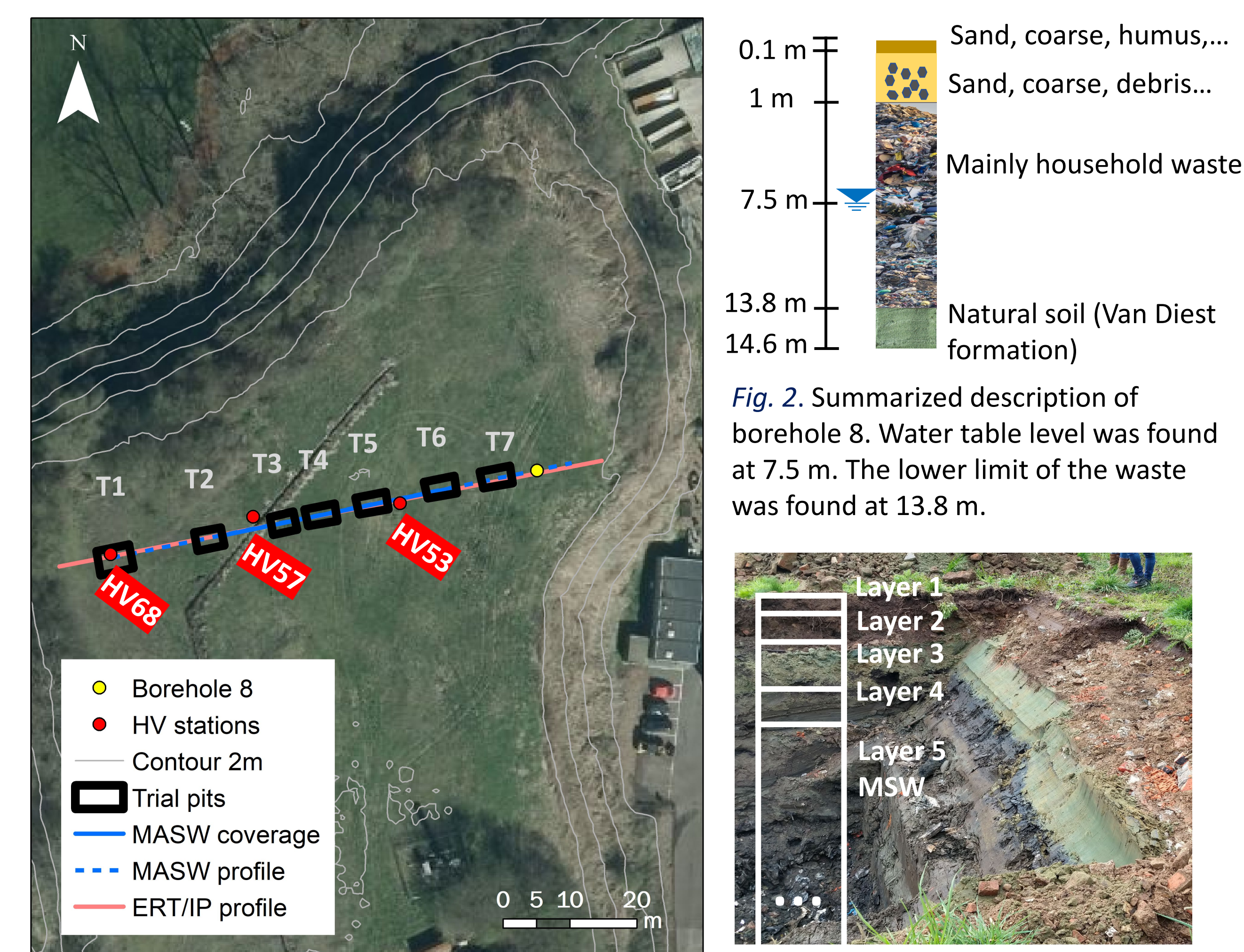
Fig. 1. Multi-geophysical survey using ERT/IP, MASW and H/V co-located with 7 trial pits (black squares) and one borehole (yellow dot). (Aerial image from Geopunt Flanders).

Legend:
- Borehole 8
- HV stations
- Contour 2m
- Trial pits
- MASW coverage
- MASW profile
- ERT/IP profile

Fig. 2. Summarized description of borehole 8. Water table level was found at 7.5 m. The lower limit of the waste was found at 13.8 m.

0.1 m — Sand, coarse, humus...
1 m — Sand, coarse, debris...
7.5 m — Mainly household waste
13.8 m / 14.6 m — Natural soil (Van Diest formation)

Fig. 3. Illustration of the 4 layers that were identified on the top of the waste in all the trial pits. The 3 dots represent that the waste extends beyond the trial pits' depths.

Layer 1 / Layer 2 / Layer 3 / Layer 4 / Layer 5 MSW
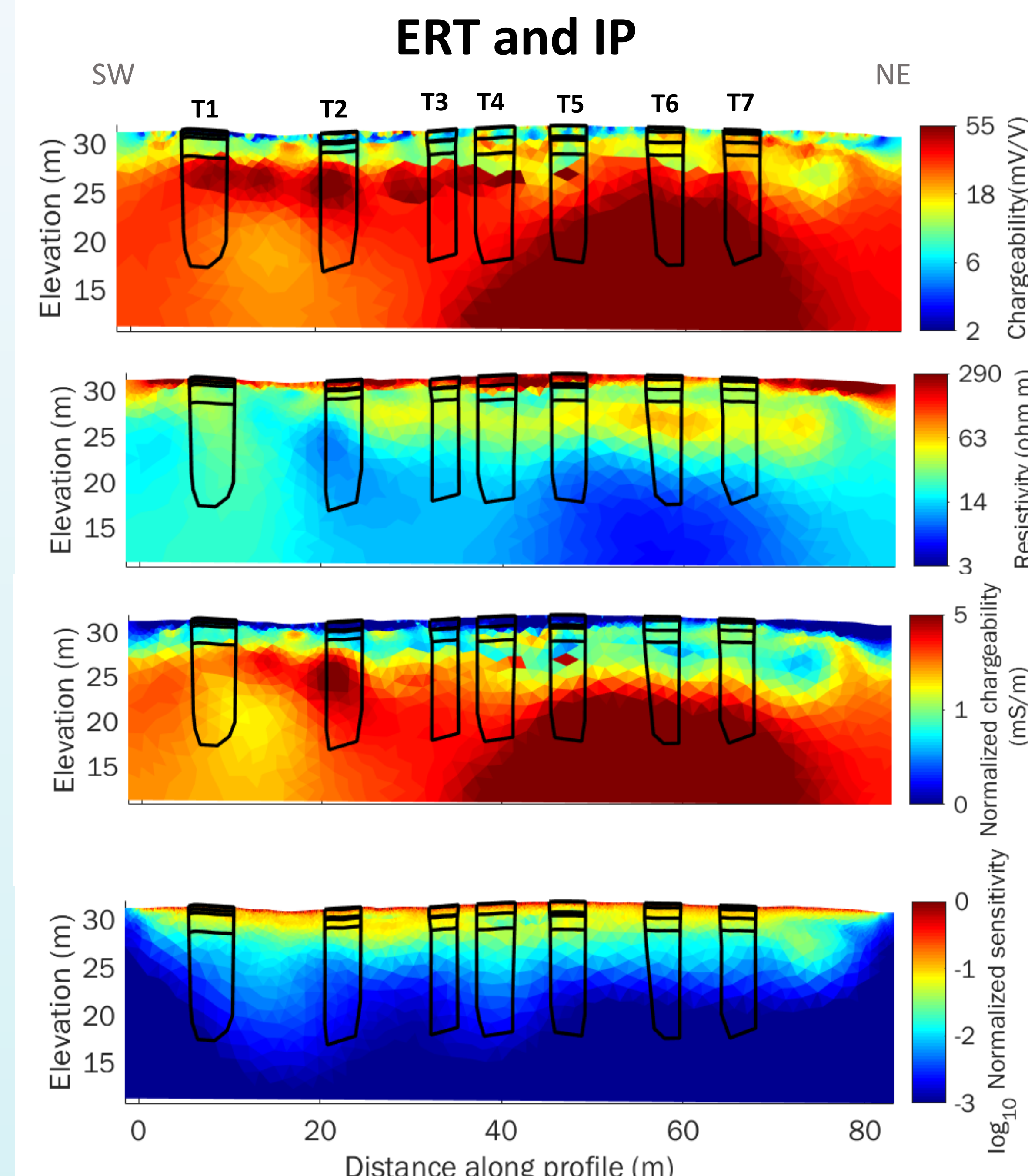
3) Methods

ERT and IP

Fig. 4. From top to bottom: the chargeability, resistivity, normalized chargeability (Slater & Lesmes, 2002) and the sensitivity models. The trial pits and identified layers are shown in black polygons (the deeper limit is extrapolated from B8).

Survey: Measurements were collected with 111 electrodes with a separation of 0.75 m using a dipole-dipole array with the 'n' factor limited to 6. The current was injected for 2s and the voltage decay was measured for 2s.

Processing: The data were inverted in BERT (Günther et al. 2006 & Rücker et al. 2006) and converged to a χ^2=0.31, rms=3.96 for the ERT data and χ^2=0.27, rms=0.41 for IP.

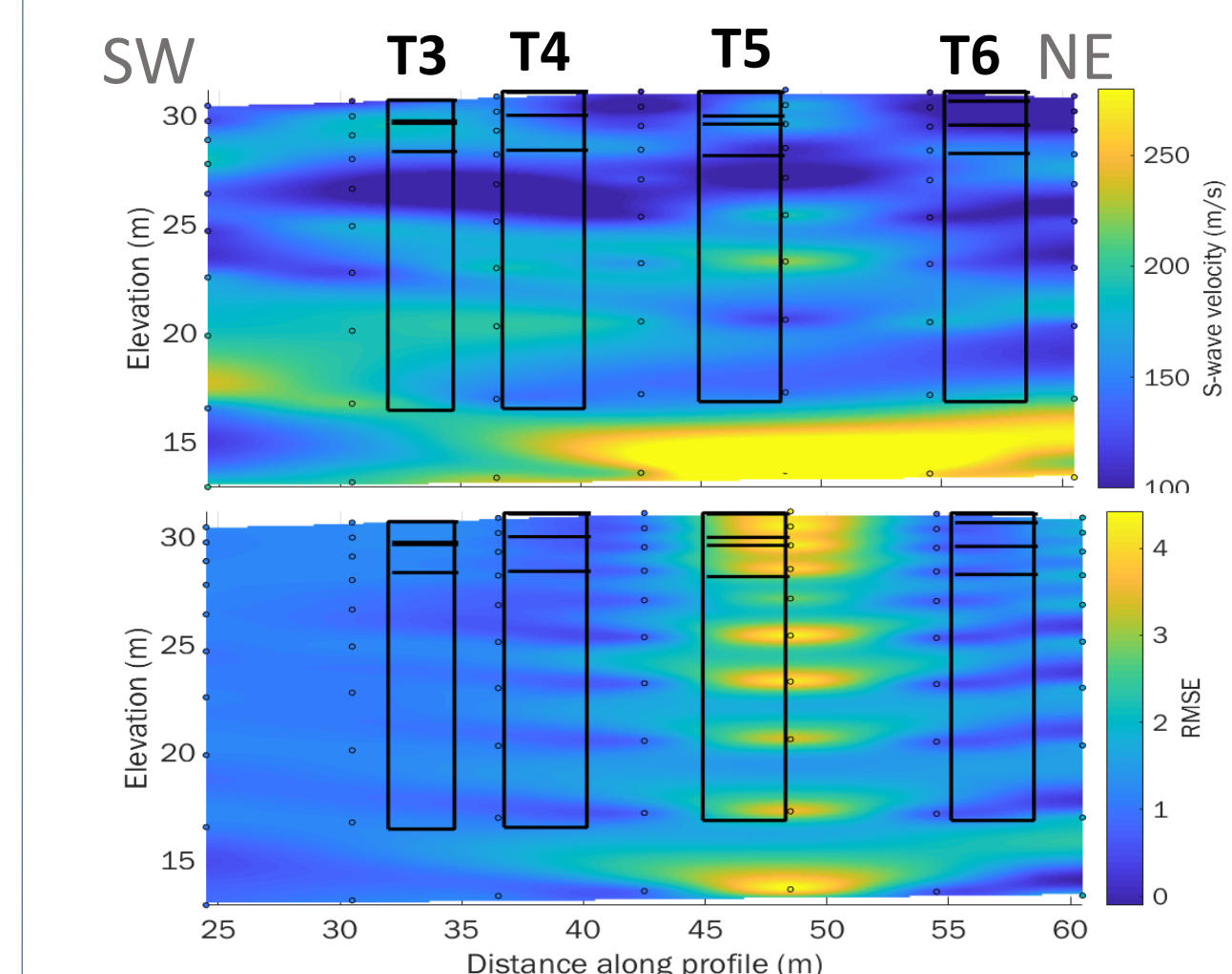### Seismic data

Active source: MASW

Fig. 5. S-wave velocity model from MASW using Rayleigh-wave dispersion data (top). Associated RMSE (bottom). The trial pits and identified layers are shown in black squares.

Survey: We used 48 vertical geophones (3.5 Hz & 10 Hz) deployed with a 1.5 m spacing and a P-wave hammer source with an offset of 6 m (fixed array).

Processing: The data were inverting emulating a roll-along acquisition in SurfSeis 6.0 (Kansas Geological survey, KGS). In Fig. 5 the circles represent the locations of the dispersion curves values.

Passive source: H/V

Instrumentation: We used a Lennartz seismometer LE-3Dlite Mk111 (3 components, 1s eigenperiod, 200 Hz sampling rate).

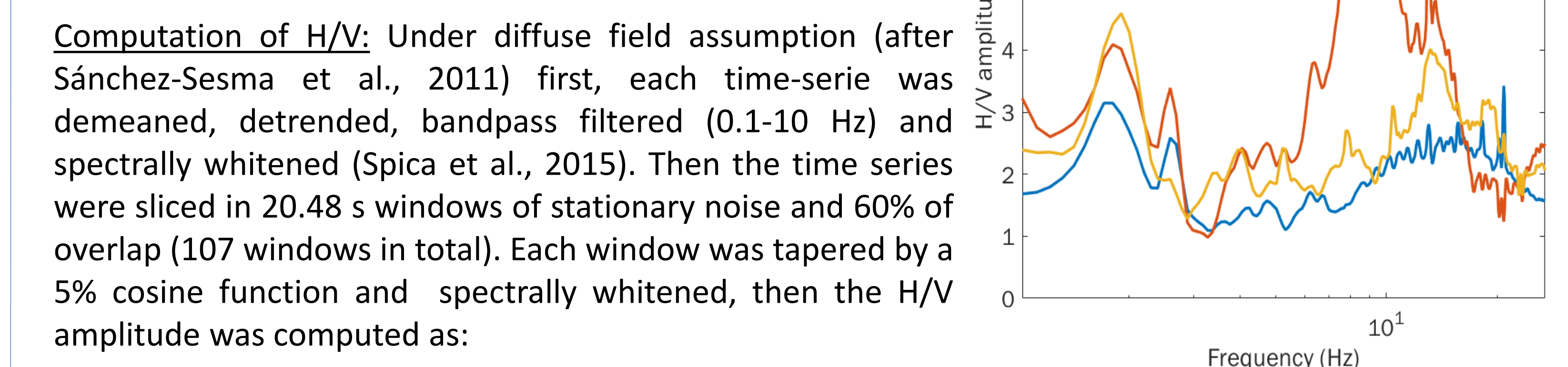Survey: Recordings of ambient noise were acquired at different positions during 15 min.

Computation of H/V: Under diffuse field assumption (after Sánchez-Sesma et al., 2011) first, each time-serie was demeaned, detrended, bandpass filtered (0.1-10 Hz) and spectrally whitened (Spica et al., 2015). Then the time series were sliced in 20.48 s windows of stationary noise and 60% of overlap (107 windows in total). Each window was tapered by a 5% cosine function and spectrally whitened, then the H/V amplitude was computed as:

$$\frac{H}{V}(w) = \sqrt{\frac{(\|u_1(x,w)\|^2) + (\|u_2(x,w)\|^2)}{(\|u_3(x,w)\|^2)}}$$

where w is the angular frequency and $u_i(x,w)$ are the displacement field components in the horizontal ($i=1,2$) and vertical ($i=3$) directions (Arai & Tokimatsu, 2004; Piña-Flores et al., 2017). The whitening consists in normalizing the signals by the source energies computed in several frequency bands (Spica et al., 2015; Perton et al., 2018).
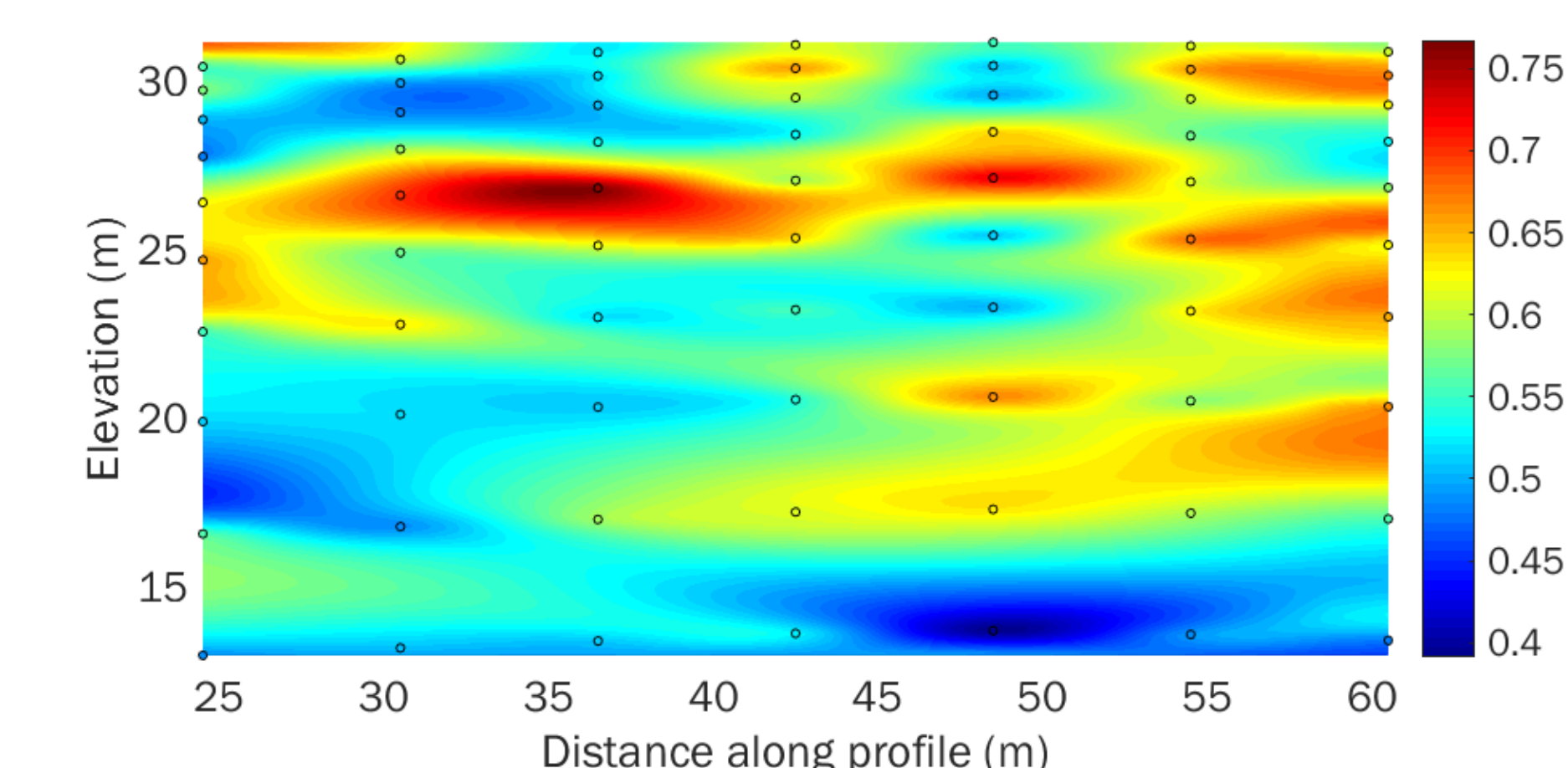
Fig. 6. Results of H/V smoothed using the LOWESS method and a span of 10 samples.

5) Permanence of ratios (τ-model): combining multiple data

This is an alternative to assess an unknown event A through its conditional probability $P(A|B,C)$ given 2 (or more) data events B, C of different sources. The permanence of ratios guarantees all limit conditions even in presence of data interdependence and can be expressed as:

$$\frac{x}{b} = \left(\frac{c}{a}\right)^{\tau(B,C)} \quad \tau(B,C) \geq 0$$

where

$$x = \frac{1-P(A|B,C)}{P(A|B,C)} \quad a = \frac{1-P(A)}{P(A)}$$

$$b = \frac{1-P(A|B)}{P(A|B)} \quad c = \frac{1-P(A|C)}{P(A|C)}$$

(Journel, 2002; MA and Jafarpour, 2019).

If the unknown event A is the waste body (Layer 5) and events B and C are the S-wave velocity and chargeability models respectively, we can use the individual conditional probabilities computed before to estimate $P(L5|V_s, chargeability)$ using co-located data from both models.

Fig. 8. Conditional probability of layer 5, given the chargeability and the S-wave model, using a τ(B,C)=0.1.

Fig. 9. Conditional probability of layer 5, given the chargeability and the S-wave model, using a τ(B,C)=0.3.

6) Conclusions and future directions

- IP method is useful to delineate MSW (plastics, paper, organics, wood, textile, metals, glass, etc.) overall. ERT is more sensitive to saturated zones within the waste and is also useful to investigate features present in the cover layer (higher sand content).
- H/V results show a low amplitude peak around 2Hz (thus it might not be reliable), however a parametric analysis at this frequency is still in agreement with the estimated thickness of the waste.
- For this case there is no clear improvement of using the τ-model for combining the chargeability and S-wave velocity models mostly due to the heterogeneity of the latter.

Ongoing work:
- Processing and inversion of H/V data using HVInv (Piña-Flores, 2015).

7) Key references

- Günter et al., 2006, . 3-d modeling and inversion of DC resistivity data incorporating topography - Part II: Inversion, GJI
- Hermans T. and Irving J., Facies discrimination with ERT using a probabilistic methodology: effect of sensitivity and regularization, NSG, 2017.
- Sánchez-Sesma et al., A theory for microtremor H/V spectral ratio: application for a layered medium, GJI, 2011.
- Spica et al., Velocity models and site effects at Kawah Ijen volcano and Ijen caldera (Indonesia) determined from ambient noise cross-correlations and directional energy density spectral ratios, JVGR, 2015.